Research Article Vol. 5, No. 11 / November 2018 / Optica 1424

Nanoparticle sensing with a spinning resonator

Hui Jing,[1,3,*] H. Lü,[1] S. K. Özdemir,[2,6] T. Carmon,[4] and Franco Nori[3,5]

[1]Key Laboratory of Low-Dimensional Quantum Structures and Quantum Control of the Ministry of Education, Department of Physics and Synergetic Innovation Center for Quantum Effects and Applications, Hunan Normal University, Changsha 410081, China
[2]Department of Engineering Science and Mechanics, Pennsylvania State University, University Park, State College, Pennsylvania 16802, USA
[3]Theoretical Quantum Physics Laboratory, RIKEN Cluster for Pioneering Research, Wako-shi, Saitama 351-0198, Japan
[4]Mechanical Engineering, Technion—Israel Institute of Technology, Haifa, 32000, Israel
[5]Physics Department, The University of Michigan, Ann Arbor, Michigan 48109-1040, USA
[6]e-mail: sko9@psu.edu
*Corresponding author: jinghui73@foxmail.com

Received 10 July 2018; revised 12 September 2018; accepted 3 October 2018 (Doc. ID 338306); published 6 November 2018

Whispering-gallery-mode (WGM) microresonators provide a high-performance platform for measuring single nanoparticles and viruses, as well as large molecules. However, there is still room for further improving their sensitivity and detection limit, towards their theoretical limit. Here, we present a new method that enhances the performance of WGM sensors based on the mode-splitting method. We show that scatterer-induced mode splitting is significantly enhanced in a rotating resonator. This enhancement originates from the different Sagnac frequency shifts that the clockwise and counterclockwise optical fields in the resonator experience due to the rotation of the resonator. Our approach, combining Sagnac shift and mode splitting, provides a new route for enhancing the coherent optical sensing of nanoparticles with single-particle resolution. In addition, our results shed light on the studies of, e.g., topological or optoacoustic effects with rotating devices.

https://doi.org/10.1364/OPTICA.5.001424

1. INTRODUCTION

Whispering-gallery-mode (WGM) optical resonators with their high quality factors and small mode volumes, enabling strong light–matter interactions, have become a versatile platform for fundamental studies and technological applications of light and its interactions with matter [1,2]. A prominent example, closely related to the present study, is ultrasensitive detection of, e.g., weak forces [3], displacement [4], and magnetic field [5] with WGM resonators. In particular, label-free and self-referenced WGM sensing of nano-objects based on mode splitting (i.e., splitting of a resonance mode into two resonances with different frequencies and linewidths) induced by a nano-object entering the mode volume of the resonator has emerged as a promising new technology with widespread applications in, e.g., medical diagnosis and environmental monitoring [6–9]. This technique can accurately count and size nanoparticles as small as 10 nm in radius, with also superior suppression of noises (such as frequency fluctuation, thermal or back-action noise, and motional disturbance) [8,10]. To further improve the sensitivity of WGM sensors, considerable efforts have been made towards suppressing losses, decreasing the resonator mode volume, or utilizing topological degeneracies arising from the non-Hermiticity of the waveguide-coupled resonators, such as recent experiments utilizing plasmonic particles [11–13], optical gain [10,14], or exceptional points [15–19].

Here, we show that the performance of a WGM nanoparticle detector can be enhanced by utilizing relativistic motional effects of light, without the need for loss compensation or WGM–plasmon hybrid structures. Specifically, we utilize the Sagnac effect, which induces *opposite* frequency shifts to counterpropagating optical modes in a spinning resonator [20], to further *enhance* the scatterer-induced mode splitting. Sagnac- and rotation-induced effects have been theoretically and experimentally investigated for, e.g., sensitive measurements of angular velocity of the medium in optical gyroscopes [21,22], optical chiral symmetry breaking [23], rotational Doppler effect [24], rotary photon drag [25], nonreciprocal light or sound propagation [26,27], and magnetometry [28]. However, the possible role of a rotating WGM resonator in single-particle sensors has not yet been explored, to the best of our knowledge. Our scheme is experimentally accessible, as the required experimental techniques and platforms are readily available [8,18,22]. Also our method is compatible with existing WGM-sensing techniques and thus, besides an additional Sagnac-induced increase in mode splitting, advantages of the WGM sensors as demonstrated in Refs. [8,10], such as self-referencing, ultrasensitivity to perturbations, fast detection, and immunity to thermal drift and laser noise [10,26,29,30], can be integrated into our proposed method.

2. RESULTS AND DISCUSSION

A. Model and Working Principle of a Spinning Nanoparticle-Detector

We consider a waveguide-coupled WGM optical resonator with a single nanoparticle (or scatterer) in its mode volume, as shown in Fig. 1(a). This resonator, with optical resonance frequency ω_a and intrinsic loss γ_a, is probed with an optical field at frequency ω_l, which is input in the clockwise (CW) direction [i.e., no input field in the counterclockwise (CCW) direction]. Here, the resonator is rotated, and the waveguide is stationary. Such a system with a spinning resonator and stationary waveguide was experimentally realized in a recent work by Maayani *et al.* who also showed that such a system can be used for optical nonreciprocity [26]. In the experiment, a resonator with radius $R = 1.1$ mm was mounted on a turbine, which spins the resonator stably around its axis, reaching the rotation frequency 6.6 kHz [26]. By positioning the resonator near a single-mode fiber, the light can be evanescently coupled into or out of the resonator through the tapered region. The spinning resonator drags air into the region between the taper and the cavity, so that a boundary layer of air forms. Due to the air pressure on the surface of the taper that faces the resonator, the taper flies above the cavity, the position of which can be self-adjusted [26], leading to stable resonator–fiber coupling. The particle in the evanescent field of the resonator acts as a scatterer, inducing the coupling of CW and CCW propagating modes with strength J and thus leading to an optical mode splitting [8]. Mode splitting induced by other factors such as surface roughness or material inhomogeneity can be pre-detected and thus minimized [8,10,26], or modes and resonators without such intrinsic mode splitting can be used. We note that by directly revealing particle polarizability (a parameter depending on the size, shape, and refractive index of the particle) [8], this technique can discriminate between particles of the same size but different refractive indices or shapes [8,10].

The CW and CCW modes in the spinning resonator experience different refractive indices [26], i.e., $n_\pm = n[1 \pm R\Omega(n^{-2} - 1)/c]$, where n and R denote, respectively, the refractive index and the radius of the resonator, Ω is the rotation speed, and c is the speed of light in vacuum. As a result, the frequencies of CW and CCW modes of a resonator experience Sagnac–Fizeau shifts [31], i.e., $\omega_a \to \omega_a \pm \Delta_{\text{sag}}$, with

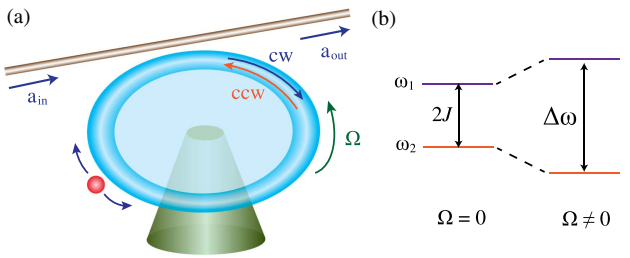

Fig. 1. (a) Schematic of a single nanoparticle sensor with a spinning resonator. The resonator with rotation speed Ω is driven by an optical field. A nanoparicle placed in the mode volume of the resonator induces a coupling with strength J between the CW and CCW modes. (b) Schematic of the energy levels of the optical eigenmodes. The frequency splitting of $2J$ for a stationary resonator ($\Omega = 0$) is increased by the Sagnac effect to $\Delta\omega > 2J$ when the resonator is spinning ($\Omega \neq 0$).

$$\Delta_{\text{sag}} = \frac{nR\Omega\omega_a}{c}\left(1 - \frac{1}{n^2} - \frac{\lambda}{n}\frac{dn}{d\lambda}\right), \tag{1}$$

where λ is the wavelength of the probe light. The dispersion term $\lambda dn/nd\lambda$ makes up 1% of the value of $(1 - 1/n^2)$, which characterizes the relativistic origin of the Sagnac effect [31]. The underlying physics is indeed well known [31]; however, the possibility of using it to enhance the performance of a particle sensor has not been explored previously.

In the rotating frame at the frequency ω_l of the probing field, the effective Hamiltonian of the system in the traveling-wave basis can be written as [8,15]

$$H_{\text{eff}} = (\Delta_+ - i\gamma)a_{\text{cw}}^\dagger a_{\text{cw}} + (\Delta_- - i\gamma)a_{\text{ccw}}^\dagger a_{\text{ccw}} + (J - i\gamma_c)a_{\text{cw}}^\dagger a_{\text{ccw}} + (J - i\gamma_c)a_{\text{ccw}}^\dagger a_{\text{cw}} + i\sqrt{\gamma_{\text{ex}}}\, a_{\text{in}}(a_{\text{cw}}^\dagger - a_{\text{cw}}), \tag{2}$$

with

$$\Delta_\pm = \Delta_a + J \pm \Delta_{\text{sag}}, \qquad \gamma = (\gamma_a + \gamma_{\text{ex}})/2 + \gamma_c, \tag{3}$$

where γ is the total optical loss, a_{cw} or a_{ccw} denotes the intracavity field of the CW or CCW mode, $\Delta_a = \omega_a - \omega_l$, γ_{ex} is the waveguide–resonator coupling rate, γ_c denotes the optical loss induced by the particle, and a_{in} is the amplitude of the probe field. The last term in Eq. (2) implies that the optical field is input only in the CW direction. The system studied here is fully classical, and $a_{\text{cw,ccw}}$ can be treated as classical numbers. The eigenfrequencies of this system are readily derived as

$$\omega_{1,2} = \omega_a + J \pm \omega' - i(\gamma \pm \gamma'), \tag{4}$$

where

$$2\omega' = [2(D^2 + 4J^2\gamma_c^2)^{1/2} + 2D]^{1/2},$$
$$2\gamma' = [2(D^2 + 4J^2\gamma_c^2)^{1/2} - 2D]^{1/2}, \tag{5}$$

and $D = \Delta_{\text{sag}}^2 + J^2 - \gamma_c^2$. The complex optical frequency splitting is then found as $\Delta\omega = \omega_1 - \omega_2 = 2\omega' - 2i\gamma'$, which is now strongly affected by rotation speed Ω.

B. Enhanced Mode-Splitting in a Spinning Resonator

Here, we consider that the scatterer falls onto the surface of the resonator and stays on the resonator, rotating with it, similar to the particles on a stationary WGM resonator [8,10]. In the following, we compare the particle-induced mode splitting in a spinning resonator with that in a stationary resonator, assuming that the particles falling onto the surface of the stationary and spinning resonators attach to the surface and stay at their place. Figure 1(b) shows the schematic of the energy levels of optical eigenmodes, which are strongly related to the detection limit. For a stationary cavity, two orthogonal standing wave modes (SWMs) are formed by the presence of the particle. The particle is detectable if the SMWs can be resolved in the transmission spectrum. The strict condition for the resolvability of mode splitting in the transmission spectrum was previously defined as $J > \gamma$ [32], which can be generalized to $\omega' > \gamma$ for the spinning case. Also, the upper limit of the detection is $r \ll \lambda$ [8], where r is the radius of the particle. To compare the frequency splitting in a rotating system and that in a stationary system, we define the enhancement factor

$$\eta = \left|\frac{\Delta\omega(\Omega \neq 0)}{\Delta\omega(\Omega = 0)}\right| = \left[\frac{D^2 + 4J^2\gamma_c^2}{(J^2 + \gamma_c^2)^2}\right]^{1/4} > 1. \tag{6}$$

Clearly, factor η depends on the rotation speed of the resonator and the frequency splitting induced by the particle. We note that

for a stationary system, there is *no* observable splitting in the transmission spectrum if $J < \gamma_c$. Therefore, in evaluating η in Eq. (6). we restrict the discussion to the case $J > \gamma_c$ (i.e., observable splitting for the stationary resonator). Under this condition, $D^2 + 4J^2\gamma_c^2 > (J^2 + \gamma_c^2)^2$, and hence $D^2 > (J^2 - \gamma_c^2)^2$ should be satisfied to have $\eta > 1$. It is easy to show that $D^2 > (J^2 - \gamma_c^2)^2$ is always true, implying that η is always greater than one (i.e., $\eta > 1$). Thus, mode splitting in a spinning resonator (i.e., $\Omega \neq 0$) is always larger than mode splitting in a stationary resonator (i.e., $\Omega = 0$) for the same perturbation. We mention that particle position does not affect the Sagnac-induced enhancement (or change) in the splitting, but it does affect the splitting due to scatterer-induced modal coupling [8]. Thus enhancement of the Sagnac-based scheme over the stationary-resonator-based schemes utilizing mode splitting is not affected by the position of the particle. Similar to stationary sensors, the spinning sensor is also robust against additional (but detectable) noises or uncertainty of, e.g., rotation speed [22,26,28,33]. Moreover, the rotary uncertainty or the uniformity of the resonator can be optically detected and overcome via designing or calibrating the resonator and related systems [22,28,33].

Figure 2(a) shows enhancement factor η as a function of rotation speed for different particle-induced mode couplings. In our calculations, we choose experimentally available values [8,17,26], i.e., $n = 1.44$, $\omega_a = 193.5$ THz, and $\gamma_{ex} = \gamma_a = 6.43$ MHz. In Fig. 2(a), we choose $R = 1.1$ mm, $J/\gamma_a = 1.5$, and $\gamma_c/\gamma_a = 0.3$ for case A, while we choose $R = 0.5$ mm, $J/\gamma_a = 1.1$, and $\gamma_c/\gamma_a = 0.065$ for case B, as in experiments [17,18]. The values of J and γ_c depend on the radius or the refractive index of the particle, and the mode volume of the resonator [8,18]. We find that η *increases* with rotation speed Ω, leading to enhanced frequency splitting. We note that rotation speed $\Omega = 6.6$ kHz for $R = 1.1$ mm has been realized experimentally [26]; for comparisons, we also plot the case with accessible parameters $\Omega = 30$ kHz and $R = 0.5$ mm. We also note that much higher frequencies of rotation have been realized in recent experiments [34,35]. These results imply that spinning the resonator provides a potentially helpful way to further improve the performance of the particle sensor. Thus, particles that may go undetected with a stationary sensor may be detected with a spinning resonator.

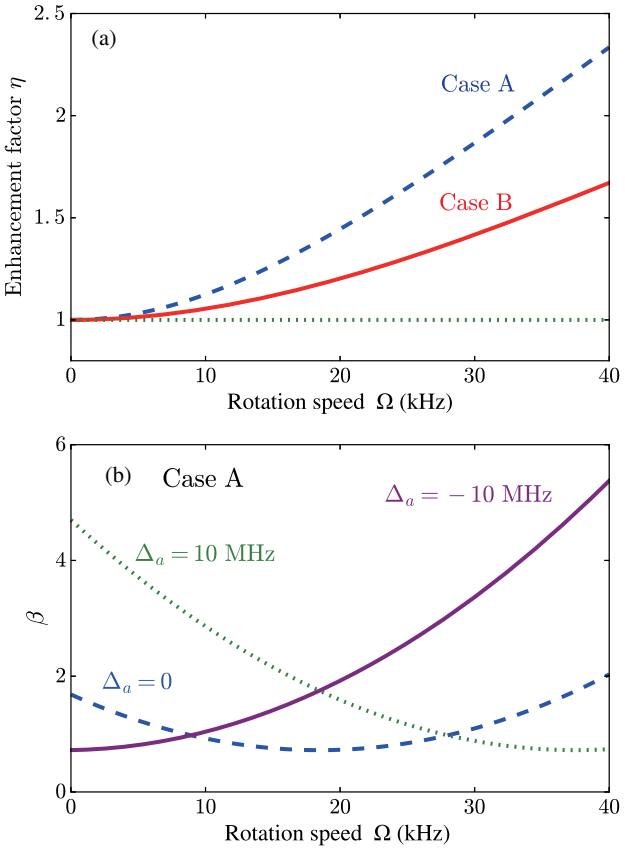

Fig. 2. Sensitivity enhancement factor η (a) and relative photon number $\beta = |\tilde{a}_{cw}|^2/|\tilde{a}_{ccw}|^2$ (b) as a function of rotation speed Ω. We choose $R = 1.1$ mm, $J/\gamma_a = 1.5$, and $\gamma_c/\gamma_a = 0.3$ for case A, and $R = 0.5$ mm, $J/\gamma_a = 1.1$, and $\gamma_c/\gamma_a = 0.065$ for case B, as in recent experiments [8,17,18]. Also, J and γ_c depend on the properties of the particle and the resonator [8,17,18].

C. Enhancement of Transmission in a Spinning Resonator

The rotation also induces resonance frequency shifts for optical modes, so that the intracavity fields can be strongly modified. To clearly see this, we derive the steady-state values of the fields in the CW and CCW directions as

$$\tilde{a}_{cw} = \frac{\sqrt{\gamma_{ex}}\, a_{in}(\gamma + i\Delta_-)}{(\gamma + i\Delta_+)(\gamma + i\Delta_-) + (J - i\gamma_c)^2},$$
$$\tilde{a}_{ccw} = -\frac{\sqrt{\gamma_{ex}}\, a_{in}(iJ + \gamma_c)}{(\gamma + i\Delta_+)(\gamma + i\Delta_-) + (J - i\gamma_c)^2}, \quad (7)$$

and define the relative photon number as

$$\beta = \frac{|\tilde{a}_{cw}|^2}{|\tilde{a}_{ccw}|^2} = \frac{\gamma^2 + (\Delta_a + J - \Delta_{sag})^2}{J^2 + \gamma_c^2}. \quad (8)$$

Figure 2(b) shows that β depends on both rotation speed Ω and optical detuning Δ_a. For $\Delta_a/J \leq -1$, β always increases with Ω, while for $\Delta_a/J > -1$, β first decreases, arriving at a minimum at $\Delta_{sag} = \Delta_a + J$, and then increases with increasing Ω. We see from Eq. (7) that the intracavity photon numbers of both the CW and CCW modes decrease with Ω, as a result of the shifted optical resonance. However, for a high rotation speed Ω, the Sagnac shift Δ_{sag} exceeds Δ_a and J, leading to a larger value of β, and thus significantly affecting the properties of light propagation.

By using the input–output relation, $a_{out} = a_{in} - \sqrt{\gamma_{ex}}\,\tilde{a}_{cw}$, where a_{out} is the amplitude of the output field, we obtain the optical transmission rate

$$T = \left|\frac{a_{out}}{a_{in}}\right|^2 = \left|1 - \frac{\gamma_{ex}(\gamma + i\Delta_-)}{(\gamma + i\Delta_+)(\gamma + i\Delta_-) + (J - i\gamma_c)^2}\right|^2. \quad (9)$$

Figures 3(a) and 3(b) show the transmission rate T for the case $\gamma_c/\gamma_a = 0.3$ (case A in Fig. 2) as a function of optical detuning. In the absence of a particle, a stationary resonator supports two degenerate modes with the same frequency but opposite propagation directions (CW and CCW traveling modes), exhibiting a resonance dip at $\Delta_a = 0$ in the transmission spectrum. When the same resonator spins at speed Ω, the resonance dip shifts to $\Delta_a = -\Delta_{sag}$ due to the Sagnac effect [blue curves in Figs. 3(a)–3(b)]. When a nanoparticle enters the mode volume of the stationary resonator, scattering-induced modal coupling leads to two orthogonal standing-wave modes, which are reflected in the transmission spectrum as two spectrally different resonances. The asymmetry in the spectrum implies that the particle induces

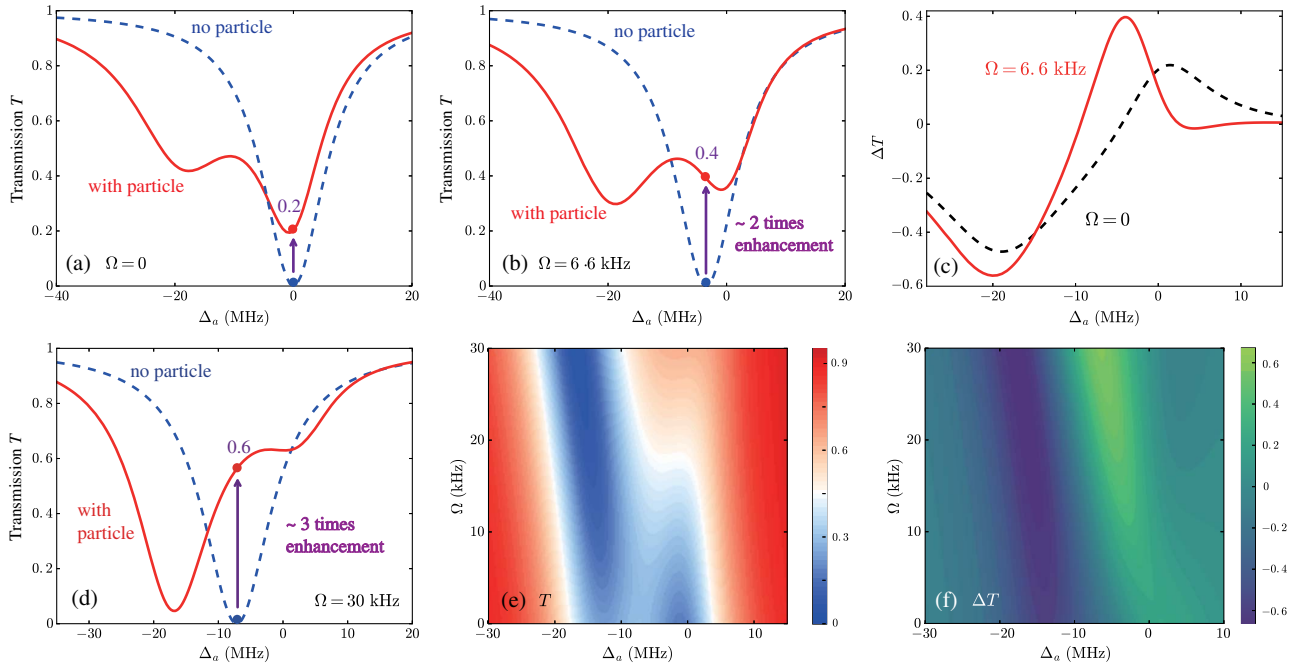

Fig. 3. Transmission rate T as a function of optical detuning Δ_a for $\Omega = 0$ (i.e., a stationary resonator) (a), $\Omega = 6.6$ kHz (b), and $\Omega = 30$ kHz (d). (c) Transmission difference ΔT as a function of optical detuning Δ_a. (e) Transmission rate T as a function of optical detuning Δ_a and rotation speed Ω. (f) Transmission difference ΔT as a function of detuning Δ_a and rotation speed Ω. We choose $R = 1.1$ mm, $J/\gamma_a = 1.5$, and $\gamma_c/\gamma_a = 0.3$ (i.e., case A in Fig. 2) in (a)–(c), and $R = 0.5$ mm, $J/\gamma_a = 1.1$, and $\gamma_c/\gamma_a = 0.065$ in (d)–(f) (i.e., case B in Fig. 2).

different losses to the two orthogonal modes. For a spinning resonator with a nanoparticle in the mode volume, the resonance dips of the split modes shift to $\Delta_a = -J \pm \omega'$. If Ω, for example, is tuned from 0 kHz to 6.6 kHz, the frequency splitting increases from 19.35 MHz to 20.51 MHz. The difference in linewidth, however, changes slightly. The resonance shift and the enhancement of frequency splitting due to Sagnac effect lead to changes in the transmission at fixed frequency detuning $\Delta_a = -\Delta_{\text{sag}}$. For example, in the presence of a particle, the change in the transmission for $\Omega = 6.6$ kHz is twice that for $\Omega = 0$, as shown in Figs. 3(a)–3(b).

We note that the location of the particle affects mode splitting due to the scatterer-induced modal coupling but not the enhancement (or change) in mode splitting due to the Sagnac effect (in a spinning resonator). In the case of mode splitting due to the scatterer-induced modal coupling, a particle located in a high-intensity field in the mode volume leads to a larger mode splitting than the same particle located in a low-intensity field in the mode volume. However, Sagnac-induced enhancement in mode splitting, depending on the spinning speed of the resonator, is the same for the particle located in the low or high field in the mode volume. Hence, in experiments it is possible to distinguish these two different kinds of effects. Also we note that the Sagnac effect can lead to an observable frequency shift of the output spectrum even for the case without any particle. Therefore, by analyzing the change of, e.g., the transmission spectra of the probe light, the additional effect induced by the scatter can also be identified by analyzing, e.g., the locations of the minima of the transmission curve.

To show the impact of the particle on light propagation in a spinning resonator, we define the transmission difference: $\Delta T = T - T_0$, where T and T_0 are the optical transmission with and without the particle, respectively. Figure 3(c) shows that for a high rotation rate, ΔT can be tuned in a large range. We note that ΔT can be changed even for a slow rotation speed. For example, for $\Delta_{\text{sag}} \ll \gamma_a, J$, we have

$$\Delta T(\Delta_a = 0) \approx \frac{J^2 + \gamma_c^2 + 2J\Delta_{\text{sag}}}{(\gamma + \gamma_c)^2 + 4J^2}. \tag{10}$$

The term $2J\Delta_{\text{sag}}$ in the numerator of Eq. (10) implies that the effect of frequency splitting on the transmission is *enhanced* by the rotation speed of the resonator. In other words, the transmission of a spinning resonator is very sensitive to perturbations induced by a particle.

Then we consider the transmission rate for the case $\gamma_c/\gamma_a = 0.065$ (case B in Fig. 2) with much higher rotation speeds. Figure 3(d) shows the transmission rate T for $\Omega = 30$ kHz. We find that compared with case A (i.e., $\gamma_c/\gamma_a = 0.065$) with $\Omega = 6.6$ kHz, the spectrum is strongly modified for higher rotation speed. If Ω is increased from 0 kHz to 30 kHz, the frequency splitting increases from 14.19 MHz to 20.13 MHz. Figure 3(e) shows the dependence of T on Δ_a and Ω. Clearly, the frequency splitting is broadened for a large value of Ω. In this regime,

$$\tilde{a}_{\text{cw}} \approx \frac{\sqrt{\gamma_{\text{ex}}}\, a_{\text{in}}}{\gamma + i(\Delta_a + J + \Delta_{\text{sag}})}$$

from which we find that the intracavity photon number of the CW mode for $\Delta_a < 0$ is larger than that for $\Delta_a > 0$. As a result, strong absorption emerges in the $\Delta_a < 0$ regime, which is in sharp contrast to the stationary system. Figure 3(f) shows that depending on both optical detuning and rotation speed, ΔT can be tuned to be positive or negative with a fixed optical detuning, indicating also a convenient way to observe the splitting induced by the particle.

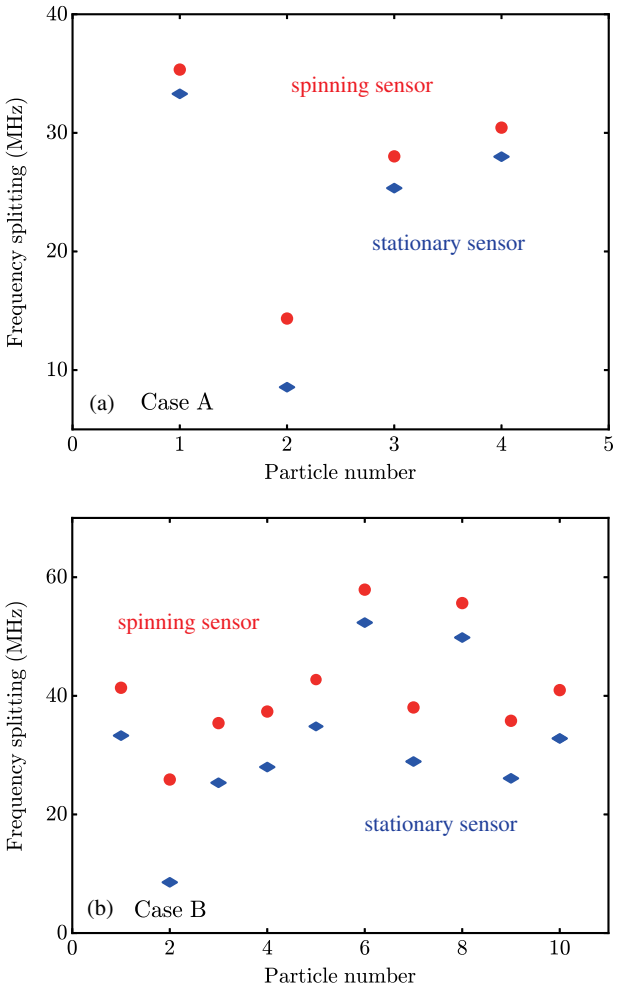

Fig. 4. Variation in frequency splitting for a spinning and a stationary WGM-based particle sensor as more than one particle is deposited on the resonators. The rotation speed is set as $\Omega = 6.6$ kHz in (a) and 30 kHz in (b).

D. Multiparticle Detection with a Spinning Resonator

The above discussion can be generalized to a more practical case with several particles falling into the mode volume one by one. In this situation, the effective Hamiltonian can be written as

$$H'_{\text{eff}} = (\Delta'_{+} - i\gamma')a^{\dagger}_{\text{cw}}a_{\text{cw}} + (\Delta'_{-} - i\gamma')a^{\dagger}_{\text{ccw}}a_{\text{ccw}} + C_1 a^{\dagger}_{\text{cw}}a_{\text{ccw}} + C_2 a^{\dagger}_{\text{ccw}}a_{\text{cw}} + i\sqrt{\gamma_{\text{ex}}}\, a_{\text{in}}(a^{\dagger}_{\text{cw}} - a_{\text{cw}}), \tag{11}$$

where

$$\Delta'_{\pm} = \Delta_a + \sum_{i=1}^{N} J_i \pm \Delta_{\text{sag}}, \quad \gamma' = (\gamma_a + \gamma_{\text{ex}})/2 + \sum_{i=1}^{N} \gamma_{c,i},$$

$$C_{1,2} = \sum_{i=1}^{N} (J_i - i\gamma_{c,i}) \exp(\mp i2m\beta_j), \tag{12}$$

where $(J_i - i\gamma_{c,i})$ and β_i are the complex frequency splitting and angular position of i-th particle, N is the particle number, and m is the azimuthal mode number. Figure 4 shows discrete up or down jumps of the frequency splitting with nanoparticles continuously deposited on the sensor, in which random values of $(J_i - \gamma_{c,i})$ and β_i are chosen. It is obvious that detection sensitivity is enhanced for each particle by spinning the resonator. We note that a higher rotation speed can be achieved for a smaller resonator, leading to further enhanced detection sensitivity, as shown in Fig. 4(b).

3. CONCLUSION

In conclusion, we have showed that spinning a WGM resonator enhances the performance of a WGM-based nanoparticle detector. Compared to a stationary sensor, our scheme features both an enhanced mode splitting and a strongly modified transmission spectrum, providing a new way to enhance the sensitivity of WGM-based particle sensors, without the need for complex materials, hybrid systems, optical gain, or low temperatures. Our proposed method is complementary to other state-of-the-art sensing techniques already achieved experimentally, using, e.g., an active resonator [10] or a sensor operating at an exceptional point [18,19].

We note that rotating resonators or sensors have been pursued very recently in various experiments [22,26,28], with precisions limited by—as also in their stationary counterparts—optical absorption, optical recoil noise, or the motion of the particles. Future works will consider the effect of various losses and noises on the performance of these sensors and an in-depth study of time-varying interaction between WGM field and the flying-by nanoparticles [8]. Finally, besides sensing, our results may potentially lead to the use of spinning resonators in engineering of, e.g., topological or optoacoustic devices.

APPENDIX A: EXPERIMENTAL FEASIBILITY OF THE SPINNING SENSOR

In our proposed scheme, the ring cavity can be mounted on a turbine, which spins the resonator, as in the recent experiment performed by Maayani *et al.* [26]. In the experiment, the resonator with radius $R = 1.1$ mm can spin with the stability of its axis, reaching the rotation frequency 6.6 kHz. By positioning the resonator near a single-mode telecommunication fiber, the light can be coupled into or out of the resonator evanescently through the tapered region.

For such a spinning device [26], the aerodynamic process plays a key role in stable resonator–fiber coupling: a fast spinning resonator can drag air into the region between the taper and the cavity, so that a boundary layer of air forms. Due to the air pressure on the surface of the taper facing the resonator, the taper flies at a height above the cavity, which can be several nanometers. If some perturbation induces the taper rising higher than the stable equilibrium height, it floats back to its original position, which is called "self-adjustment" [26]. The self-adjustment of the taper separation from the spinning resonator enables critical coupling of light into the cavity, by which counter-circulating light experiences optical drag identical in size, but opposite in sign. Importantly, this experiment confirms that the taper did not touch or stick to the rotating resonator even if the taper is pushed towards it, which is in contrast to the situation for a stationary resonator (i.e., the taper may stick to the resonator through van der Waals forces and thus needs to be pulled back to break the connection). Other factors, such as intermolecular forces, lubricant compressibility, tapered-fiber stiffness, and wrap angle of the fiber, may affect resonator–waveguide coupling. However, these factors are confirmed to be negligible in the experiment, which are thus also neglected in our discussions on the spinning sensor.

We consider that the scatterer falls onto the surface of the resonator and stays on the resonator, rotating with it, similar to the particles on a stationary WGM resonator [8,10]. We compare the mode splitting in a spinning resonator with the splitting in a stationary resonator: if the particle is not stationary on the mode volume (e.g., particle diffuses on the surface), then we will observe changes in the amount of mode splitting. If the particle is detached from the resonator due to spinning or any other reasons, then mode splitting will disappear and the transmission will return back to the case when there is no particle.

The strength of the interaction between the cavity field and the particle is affected by the location of the particle. For example, a particle may be located on a position on the resonator where there is no field, or the field is very weak. This will lead to lower interaction strength and hence the amount of mode splitting will be small. If the particle sits on a position where the field is high, then the mode splitting will be larger as the light–particle interaction strength will be higher. This effect is valid in the Sagnac-based particle detector too. However, the Sagnac effect itself is not affected by the particle position. Thus the enhancement of mode splitting originating from the Sagnac effect will not be affected by the position of the particle. However, mode splitting that originates from the scatterer-induced modal coupling is affected by the position of the particle. Therefore, the fact that the Sagnac-based scheme performs better than a stationary-resonator-based scheme utilizing mode splitting does not change by the position of the particle. The complex optical mode coupling induced by the particle, related to the overlap between the particle and mode volume of the resonator, depends on the particle position. According to Ref. [8], the complex mode coupling induced by the particle can be expressed as

$$J = -\frac{\alpha f^2(\mathbf{r})\omega_c}{2V_c}, \quad \gamma_c = \frac{2\pi^2\alpha^2 f^2(\mathbf{r})\omega_c}{3\lambda^3 V_c},$$

where $\mathbf{r}$ is the particle position, V_c is the mode volume of the resonator, $f(\mathbf{r})$ is the normalized mode distribution function, and λ is the light wavelength in the resonator. α is the particle polarizability, which depends on the size and refractive index of the particle. Then we can see that the particle position affects the values of J and γ_c, but does not change the ratio

$$\gamma_c/J = -4\pi^2\alpha/(3\lambda^3).$$

The particle position may affect detection efficiency, since the particle is undetectable if $\omega' < \gamma$ is satisfied, where ω' is half of the frequency splitting induced by the particle. However, in previous experiments [8,10], nanoparticles falling onto the stationary resonator randomly were detected and counted. Here we propose to enhance the performance of the WGM particle sensor by use of the Sagnac effect. We show that sensitivity enhancement factor η always exceeds 1 with the condition $J > \gamma_c$, which indicates an observable splitting for the stationary resonator. In Fig. 4, we also plot the frequency splitting variation for several nanoparticles, in which random values of J and γ_c are used. It is clear that the performance of a particle sensor can be enhanced by spinning the resonator.

The rotation of the resonator may lead to some mechanical effects on the particle. A fast spinning resonator drags a boundary layer of air past the region between the resonator and stationary taper, which may induce the particle diffusing in the air. This may change the overlap of the particle and the mode volume of the resonator, and then the values of J and γ_c. However, the ratio γ_c/J is not affected by the particle position. Our scheme is robust against the motion of the particle, since the sensitivity enhancement factor always exceeds 1 when there is an observable splitting in the transmission spectrum of a stationary resonator. In addition, the particle detection in current experimental WGM sensors can be very fast. We can safely say that the location of the particle and the rotation of the resonator will not change the fact that the spinning-resonator-based scheme performs better than the stationary-resonator scheme.

APPENDIX B: DERIVATION OF THE EFFECTIVE HAMILTONIAN

In consideration of the Sagnac effect, the Hamiltonian of the spinning resonator–nanoparticle system can be written as

$$\begin{aligned} H = {} & (\omega_a + \Delta_{\text{sag}})a_{\text{cw}}^\dagger a_{\text{cw}} + (\omega_a - \Delta_{\text{sag}})a_{\text{ccw}}^\dagger a_{\text{ccw}} \\ & + J(a_{\text{cw}}^\dagger a_{\text{ccw}} + a_{\text{ccw}}^\dagger a_{\text{cw}}) + \sqrt{\gamma_{\text{ex}}}\, a_{\text{in}}(a_{\text{cw}}^\dagger e^{-i\omega_l t} - a_{\text{cw}} e^{i\omega_l t}), \end{aligned}$$

where a_{cw} or a_{ccw} denotes the intracavity field of the CW or CCW mode, ω_a is the resonance frequency of the stationary cavity, ω_l is the frequency of the probe light, Δ_{sag} is the Sagnac shift, J is the optical coupling induced by the particle, γ_{ex} is the resonator–waveguide coupling rate, and a_{in} is the amplitude of the probe light. By using the unitary transformation

$$U = \exp[-i\omega_l t(a_{\text{cw}}^\dagger a_{\text{cw}} + a_{\text{ccw}}^\dagger a_{\text{ccw}})],$$

the Hamiltonian can be transformed into the rotating frame, i.e.,

$$\begin{aligned} H' &= U^\dagger H U - iU^\dagger \frac{\partial U}{\partial t}, \\ &= (\Delta_a + \Delta_{\text{sag}})a_{\text{cw}}^\dagger a_{\text{cw}} + (\Delta_a - \Delta_{\text{sag}})a_{\text{ccw}}^\dagger a_{\text{ccw}} \\ &\quad + J(a_{\text{cw}}^\dagger a_{\text{ccw}} + a_{\text{ccw}}^\dagger a_{\text{cw}}) + \sqrt{\gamma_{\text{ex}}} a_{\text{in}}(a_{\text{cw}}^\dagger - a_{\text{cw}}), \end{aligned}$$

where $\Delta_a = \omega_a - \omega_l$ is the optical detuning. Notice that the total optical loss is $\gamma = (\gamma_a + \gamma_{\text{ex}})/2 + \gamma_c$, where γ_a is the intrinsic optical loss of the resonator, and γ_c is the optical loss induced by the scatter. The effective Hamiltonian can be written as

$$\begin{aligned} H_{\text{eff}} = {} & (\Delta_+ - i\gamma)a_{\text{cw}}^\dagger a_{\text{cw}} + (\Delta_- - i\gamma)a_{\text{ccw}}^\dagger a_{\text{ccw}} + (J - i\gamma_c)a_{\text{cw}}^\dagger a_{\text{ccw}} \\ & + (J - i\gamma_c)a_{\text{ccw}}^\dagger a_{\text{cw}} + i\sqrt{\gamma_{\text{ex}}}\, a_{\text{in}}(a_{\text{cw}}^\dagger - a_{\text{cw}}), \end{aligned}$$

where $\Delta_\pm = \Delta_a \pm \Delta_{\text{sag}}$. Solving the characteristic equation of the system given by

$$(\omega_a + \Delta_{\text{sag}} - i\gamma - \omega)(\omega_a - \Delta_{\text{sag}} - i\gamma - \omega) - (J - i\gamma_c)^2 = 0,$$

we find the eigenfrequencies of the system as

$$\omega = \omega_a - i\gamma \pm \sqrt{D - 2iJ\gamma_c}, \quad D = \Delta_{\text{sag}}^2 + J^2 - \gamma_c^2.$$

By setting $D - 2iJ\gamma_c = (\omega' - i\gamma')^2$, where ω' and γ' are real numbers, we have

$$\begin{aligned} \omega' &= [(D^2 + 4J^2\gamma_c^2)^{1/2}/2 + D/2]^{1/2}, \\ \gamma' &= [(D^2 + 4J^2\gamma_c^2)^{1/2}/2 - D/2]^{1/2}. \end{aligned}$$

Then the eigenfrequencies of the system can be written as $\omega_{1,2} = \omega_a + J \pm \omega' - i(\gamma \pm \gamma')$, so that the complex mode splitting is $\Delta\omega = 2\omega' - 2i\gamma'$.

Funding. National Natural Science Foundation of China (NSFC) (11474087, 11774086); Asian Office of Aerospace Research and Development (AOARD) (FA2386-18-1-4045); Army Research Office (ARO) (W911NF-18-1-0358, W911NF-18-1-0043); MURI Center for Dynamic Magneto-Optics; Air Force Office of Scientific Research (AFOSR) (FA9550-18-1-0235, FA9550-14-1-0040); Core Research for Evolutional Science and Technology (CREST) (JPMJCR1676); Japan Society for the Promotion of Science (JSPS) (JSPS-RFBR 17-52-50023, JSPS-FWO VS.059.18N);National Science Foundation (NSF) (1807485); Pennsylvania State University (PSU), Materials Research Institute (MRI); Sir John Templeton Foundation; Israeli Centers for Research Excellence (I-CORE); RIKEN-National Institute of Advanced Industrial Science and Technology (AIST) (AIST) Challenge Research Fund.

Acknowledgment. H. J. thanks Ran Huang and Tian-Xiang Lu for their helpful discussions.

REFERENCES

1. K. J. Vahala, "Optical microcavities," Nature **424**, 839–846 (2003).
2. M. R. Foreman, J. D. Swaim, and F. Vollmer, "Whispering gallery mode," Adv. Opt. Photon. **7**, 168–240 (2015).
3. E. Gavartin, P. Verlot, and T. J. Kippenberg, "A hybrid on-chip optomechanical transducer for ultrasensitive force measurements," Nat. Nanotechnol. **7**, 509–514 (2012).
4. R. Schilling, H. Schütz, A. H. Ghadimi, V. Sudhir, D. J. Wilson, and T. J. Kippenberg, "Near-field integration of a SiN nanobeam and a SiO_2 microcavity for Heisenberg-limited displacement sensing," Phys. Rev. Appl. **5**, 054019 (2016).
5. S. Forstner, S. Prams, J. Knittel, E. D. van Ooijen, J. D. Swaim, G. I. Harris, A. Szorkovszky, W. P. Bowen, and H. Rubinsztein-Dunlop, "Cavity optomechanical magnetometer," Phys. Rev. Lett. **108**, 120801 (2012).
6. A. M. Armani, R. P. Kulkarni, S. E. Fraser, R. C. Flagan, and K. J. Vahala, "Label-free, single-molecule detection with optical microcavities," Science **317**, 783–787 (2007).
7. F. Vollmer, S. Arnold, and D. Keng, "Single virus detection from the reactive shift of a whispering-gallery mode," Proc. Natl. Acad. Sci. USA **105**, 20701–20704 (2008).
8. J. Zhu, S. K. Ozdemir, Y.-F. Xiao, L. Li, L. He, D.-R. Chen, and L. Yang, "On-chip single nanoparticle detection and sizing by mode splitting in an ultrahigh-Q microresonator," Nat. Photonics **4**, 46–49 (2010).
9. L. He, Ş. K. Özdemir, J. Zhu, W. Kim, and L. Yang, "Detecting single viruses and nanoparticles using whispering gallery microlasers," Nat. Nanotechnol. **6**, 428–432 (2011).
10. Ş. K. Özdemir, J. Zhu, X. Yang, B. Peng, H. Yilmaz, L. He, F. Monifi, S. H. Huang, G. L. Long, and L. Yang, "Highly sensitive detection of nanoparticles with a self-referenced and self-heterodyned whisperinggallery Raman microlaser," Proc. Natl. Acad. Sci. USA **111**, E3836 (2014).
11. S. I. Shopova, R. Rajmangal, S. Holler, and S. Arnold, "Plasmonic enhancement of a whispering-gallery-mode biosensor for single nanoparticle detection," Appl. Phys. Lett. **98**, 243104 (2011).
12. V. R. Dantham, S. Holler, C. Barbre, D. Keng, V. Kolchenko, and S. Arnold, "Label-free detection of single protein using a nanoplasmonic-photonic hybrid microcavity," Nano Lett. **13**, 3347–3351 (2013).
13. M. D. Baaske, M. R. Foreman, and F. Vollmer, "Single-molecule nucleic acid interactions monitored on a label-free microcavity biosensor platform," Nat. Nanotechnol. **9**, 933–939 (2014).
14. B.-B. Li, W. R. Clements, X.-C. Yu, K. Shi, Q. Gong, and Y.-F. Xiao, "Single nanoparticle detection using split-mode microcavity Raman lasers," Proc. Natl. Acad. Sci. USA **111**, 14657–14662 (2014).
15. J. Wiersig, "Enhancing the sensitivity of frequency and energy splitting detection by using exceptional points: application to microcavity sensors for single-particle detection," Phys. Rev. Lett. **112**, 203901 (2014).
16. J. Wiersig, "Sensors operating at exceptional points: general theory," Phys. Rev. A **93**, 033809 (2016).
17. B. Peng, Ş. K. Özdemir, M. Liertzer, W. Chen, J. Kramer, H. Yilmaz, J. Wiersig, S. Rotter, and L. Yang, "Chiral modes and directional lasing at exceptional points," Proc. Natl. Acad. Sci. USA **113**, 6845–6850 (2016).
18. W. Chen, Ş. K. Özdemir, G. Zhao, J. Wiersig, and L. Yang, "Exceptional points enhance sensing in an optical microcavity," Nature **548**, 192–196 (2017).
19. H. Hodaei, A. U. Hassan, S. Wittek, H. Garcia-Gracia, R. El-Ganainy, D. N. Christodoulides, and M. Khajavikhan, "Optically levitated nanodumbbell torsion balance and GHz nanomechanical rotor," Nature **548**, 187–191 (2017).
20. E. J. Post, "Sagnac effect," Rev. Mod. Phys. **39**, 475–481 (1967).
21. W. W. Chow, J. Gea-Banacloche, L. M. Pedrotti, V. E. Sanders, W. Schleich, and M. O. Scully, "The ring laser gyro," Rev. Mod. Phys. **57**, 61–104 (1985).
22. J. Li, M.-G. Suh, and K. Vahala, "Microresonator Brillouin gyroscope," Optica **4**, 346–348 (2017).
23. R. Sarma, L. Ge, J. Wiersig, and H. Cao, "Rotating optical microcavities with broken chiral symmetry," Phys. Rev. Lett. **114**, 053903 (2015).
24. M. P. J. Lavery, F. C. Speirits, S. M. Barnett, and M. J. Padgett, "Detection of a spinning object using light's orbital angular momentum," Science **341**, 537–540 (2013).
25. S. Franke-Arnold, G. Gibson, R. W. Boyd, and M. J. Padgett, "Rotary photon drag enhanced by a slow-light medium," Science **333**, 65–67 (2011).
26. S. Maayani, R. Dahan, Y. Kligerman, E. Moses, A. U. Hassan, H. Jing, F. Nori, D. N. Christodoulides, and T. Carmon, "Flying couplers above spinning resonators generate irreversible refraction," Nature **558**, 569–572 (2018).
27. R. Fleury, D. L. Sounas, C. F. Sieck, M. R. Haberman, and A. Alù, "Sound isolation and giant linear nonreciprocity in a compact acoustic circulator," Science **343**, 516–519 (2014).
28. A. A. Wood, E. Lilette, Y. Y. Fein, A. Stacey, N. Tomek, L. P. McGuinness, L. C. L. Hollenberg, R. E. Scholten, and A. M. Martin, "Quantum measurement of a rapidly rotating spin qubit in diamond," Sci. Adv. **4**, eaar7691 (2018).
29. J. D. Swaim, J. Knittel, and W. P. Bowen, "Detection of nanoparticles with a frequency locked whispering gallery mode microresonator," Appl. Phys. Lett. **102**, 183106 (2013).
30. J. Knittel, J. D. Swaim, D. L. McAuslan, G. A. Brawley, and W. P. Bowen, "Back-scatter based whispering gallery mode sensing," Sci. Rep. **3**, 2974 (2013).
31. G. B. Malykin, "The Sagnac effect: correct and incorrect explanations," Phys. Usp. **43**, 1229–1252 (2000).
32. Ş. K. Özdemir, J. Zhu, L. He, and L. Yang, "Estimation of Purcell factor from mode-splitting spectra in an optical microcavity," Phys. Rev. A **83**, 033817 (2011).
33. A. A. Wood, E. Lilette, Y. Y. Fein, V. S. Perunicic, L. C. L. Hollenberg, R. E. Scholten, and A. M. Martin, "Magnetic pseudo-fields in a rotating electron–nuclear spin system," Nat. Phys. **13**, 1070–1073 (2017).
34. R. Reimann, M. Doderer, E. Hebestreit, R. Diehl, M. Frimmer, D. Windey, F. Tebbenjohanns, and L. Novotny, "Enhanced sensitivity at higher-order exceptional points," Phys. Rev. Lett. **121**, 033602 (2018).
35. J. Ahn, Z. Xu, J. Bang, Y.-H. Deng, T. M. Hoang, Q. Han, R.-M. Ma, and T. Li, "GHz rotation of an optically trapped nanoparticle in vacuum," Phys. Rev. Lett. **121**, 033603 (2018).